archives
of thermodynamics
Vol. **44**(2023), No. 2, 177–194
DOI: 10.24425/ather.2023.146564

Analysis of heat and mass transfer in an adsorption bed using CFD methods

SZYMON JANUSZ[a,b*]
MACIEJ SZUDAREK[c]
LESZEK RUDNIAK[d]
MARCIN BORCUCH[b]

[a] Cracow University of Technology, Jana Pawla II 37, 31-864 Kraków, Poland

[b] M.A.S. Sp z o.o., Research and Development Department, Składowa 34, 27-200 Starachowice, Poland

[c] Warsaw University of Technology, Institute of Metrology and Biomedical Engineering, św. Andrzeja Boboli 8, 02-525 Warszawa, Poland

[d] Warsaw University of Technology, Faculty of Chemical and Process Engineering, Waryńskiego 1, 00-645 Warszawa, Poland

Abstract The trend of reducing electricity consumption and environmental protection has contributed to the development of refrigeration technologies based on the thermal effect of adsorption. This article proposes a methodology for conducting numerical simulations of the adsorption and desorption processes. Experimental data available in the literature were used as guidelines for building and verifying the model, and the calculations were carried out using commercial computational fluid dynamics software. The simulation results determined the amount of water vapor absorbed by the adsorbent bed and the heat generated during the adsorption process. Throughout the adsorption process, the inlet water vapor velocity, temperature, and pressure in the adsorbent bed were monitored and recorded. The results obtained were consistent with the theory in the literature and will serve as the basis for further, independent experimental studies. The validated model allowed for the analysis of the effect of cooling water temperature on the sorption capacity of the material and the effect of heating water temperature on bed regeneration. The proposed approach can be useful in

*Corresponding Author. Email: szymon.janusz@doktorant.pk.edu.pl

analyzing adsorption processes in refrigeration applications and designing heat and mass exchangers used in adsorption systems.

Keywords: Heat transfer; Adsorption; CFD; Mass transfer; Refrigeration devices

Nomenclature

a	–	amount of adsorbed water vapor, kg/kg
a_{eq}	–	equilibrium concentration, kg/kg
C	–	coefficient of inertial resistance, 1/m
c_p	–	specific heat capacity, J/kgK
D_e	–	effective diffusion coefficient, m^2/s
D_p	–	diameter of the bed particles, m
D_0	–	kinematic diffusion coefficient, m^2/s
E_a	–	activation energy, J/mol
H	–	heat of adsorption, J/kg
k	–	thermal conductivity of the medium
k_m	–	LDF model coefficient, 1/s
P	–	pressure, Pa
P_s	–	saturation pressure, Pa
P_v	–	absolute pressure, Pa
Q	–	energy source term, W/m^3
R	–	gas constant, J/(molK)
r_a	–	radius of bed particles, m
S_i	–	source term of momentum, N/m^3
S_m	–	source term of mass, $kg/(s\ m^3)$
T	–	temperature, K
v	–	velocity, m/s
v_i	–	Cartesian components of velocity in x_i-direction
x_i	–	Cartesian coordinates, m

Greek symbols

α	–	permeability, m^2
ε	–	porosity of the medium
μ	–	dynamic viscosity of the medium, Pa·s
ρ	–	density of the medium, kg/m^3
τ	–	time, s

Subscripts

b	–	adsorption bed
c	–	cooling water
f	–	fluid
h	–	heating water
i, j	–	components
s	–	solid
sc	–	single cycle
v	–	vapor

Abbreviations

ads	–	adsorption/
CFD	–	(computational fluid dynamics
COP	–	coefficient of performance
des	–	desorption

1 Introduction

As a result of the increasing demand for heating, cooling, and air conditioning over the last century, numerous refrigeration technologies have been developed. Compressor cooling systems dominate the market due to their high coefficient of performance (COP). Although these devices perform well in terms of heating and cooling, they have a negative impact on the environment. This is due to the refrigerants (such as freon, propane, and carbon dioxide) used in compressor devices, which have a negative impact on the ozone layer and global warming. The mentioned refrigerants, despite the reduction of the global warming potential parameter, are still more harmful to the environment than, for example, water. Additionally, refrigeration devices account for approximately 20% of worldwide electrical energy used in buildings [1]. Technologies based on sorption processes are free of the drawbacks mentioned above [2]. One of these technologies is adsorption.

Adsorption cooling systems operate on environmentally friendly refrigerants (such as water) and allow to recover waste heat, thus to reduce primary energy consumption [3]. Furthermore, adsorption systems are characterized by low operating and maintenance costs, lack of vibration, and quiet operation [4]. Despite their numerous advantages, adsorption cooling systems also have drawbacks, such as intermittent operation, large equipment size, the need for vacuum maintenance, and, above all, low COP [5]. Therefore, there are ample opportunities for research to improve the efficiency of adsorption systems.

To provide continuous cooling production, adsorption cooling devices must be equipped with at least two beds. When a refrigerant is adsorbed in one bed, the other bed undergoes regeneration or desorption. The cycle starts with the refrigerant vaporizing in the evaporator. As a result of refrigerant vaporization, heat is being drawn from the water flowing through the heat exchanger, and cooling water is produced as a result [6]. The operating conditions of the process are closely related to the required parameters of cooling water.

In the case of using water as a refrigerant, it is necessary to maintain a very low working pressure of the unit, as for water temperature of 280 K (7°C) the saturation pressure is 1000 Pa. This poses additional requirements regarding the construction of adsorption equipment – it must be sufficiently airtight to maintain low pressure. During evaporation, the evaporator is connected to a chamber where an adsorption bed is located. The produced vapor is adsorbed by the bed, which makes it possible to maintain low pressure in the evaporator. The adsorption chamber is not connected to the condenser at this stage. When the adsorption bed becomes saturated, the evaporator chamber is disconnected, and the regeneration process of the bed begins. A working fluid at an elevated temperature is supplied to the adsorption bed to force the desorption of refrigerant molecules from the adsorbent pores. After a certain period called switching time, the connection with the condenser chamber is opened. This stage is called the desorption stage. After condensation, the refrigerant flows to the evaporator, where the next cycle of the device operation begins [7].

Adsorption technology is based on surface sorption phenomena. In the case of refrigeration devices, water is most commonly used as the adsorbate, as it is a chemically stable and environmentally friendly liquid. Porous materials with a developed active surface area (such as silica gels) are used as adsorbents. Adsorbate molecules are trapped in the adsorbent pores by van der Waals forces (weak intermolecular electrostatic bonds). According to the law of conservation of mass, the mass of the adsorbent (porous material) changes, while the adsorbate (refrigerant) only changes its state and condenses on the porous surface of the adsorbent [8]. As a result, energy called adsorption heat is released. This means that adsorption is an exothermic phenomenon, and it is necessary to cool the bed for the process to proceed properly. This is an essential element of the process that affects its efficiency [9]. Similarly, desorption is an endothermic process, so to regenerate a saturated adsorption bed, energy must be supplied from outside. This is one of the reasons why adsorption aggregates have a low COP coefficient, but they are still used in places where waste low-temperature heat can be utilized.

The significant influence of heating and cooling the bed on the efficiency of the adsorption process requires intensive energy exchange between the adsorbent and the heating/cooling source. This is one of the main design challenges for adsorption heat exchangers. Additionally, the temperature distribution in the exchanger should be as uniform as possible, and the pressure drops of the working fluid should be minimized. Numerical simu-

lations using CFD (computational fluid dynamics) are increasingly used to optimize such devices, e.g. improve the geometry of the exchanger [10, 11], determine the optimal cycle time of the device [12], or determine the effect of the adsorbent size on the sorption capacity and heat exchange in the adsorption bed [13].

Modelling the adsorption process using CFD poses several challenges. Fine-grained adsorbent materials generate a significant number of computational elements, making calculations infeasible. Therefore, simplifying the model is necessary by replacing the adsorbent bed with a porous material, which requires determining the substitute characteristics of the porous material. Another challenge is the selection of appropriate equilibrium equations, process kinetics, and their implementation method. Each adsorbent-adsorbate pair has unique features, which means that developed models are not universal.

In this paper, a methodology for simulating mass and heat transfer in an adsorbent bed is presented, which is then validated against available experimental data [14]. The influence of the cooling water temperature on the sorption capacity of silica gel and the dependence of the cooling device's operating cycle on the cooling water temperature are shown.

2 Method and results

The analyzed sample consisted of a heat exchanger with an insulated aluminium housing filled with silica gel (Fig. 1). The geometry was simplified for computational purposes and consisted of only two elements, as shown in Fig. 2: the adsorption bed and the water vapor volume. The heat exchanger was replaced by a convective boundary condition with a heat transfer coefficient of 600 W/m^{2}K and a temperature of 303 K. An adiabatic boundary

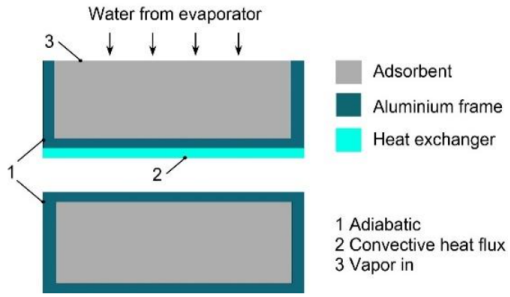

Figure 1: Experimental setup diagram, based on [14].

condition replaced the aluminum frame. The computational mesh which consists of 537 600 hexahedral cells is presented in Fig. 3.

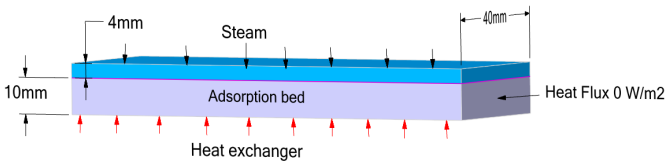

Figure 2: Simplified geometry used in the simulation.

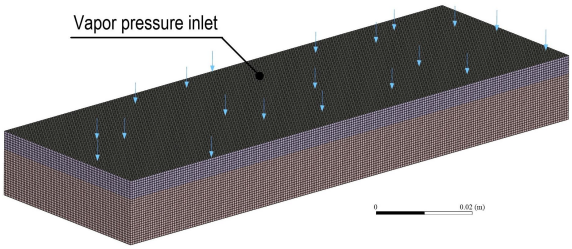

Figure 3: View of the numerical mesh of the studied sample.

The calculations were carried out using commercial computational fluid dynamics software Ansys Fluent [15] in which unsteady Navier-Stokes equations and energy conservation equation were solved using the finite volume method, assuming laminar flow and using superficial velocity formulation. Thermal equilibrium between the adsorption bed (porous medium) and the fluid was assumed:

$$\frac{\partial \rho_f}{\partial \tau} + \frac{\partial (\rho_f v_i)}{\partial x_i} = -S_m \rho_s \frac{1-\varepsilon}{\varepsilon}\,, \tag{1}$$

$$\rho\left(\frac{\partial v_i}{\partial \tau} + v_j \frac{\partial v_i}{\partial x_j}\right) = \frac{\partial P}{\partial x_i} + \mu\left[\left(\frac{\partial v_i}{\partial x_j} + \frac{\partial v_j}{\partial x_i}\right) - \frac{2}{3}\frac{\partial}{\partial x_i}\left(\frac{\partial v_k}{\partial x_k}\right)\right] + S_i\,, \tag{2}$$

$$\left[(\rho c_p)_s (1-\varepsilon) + (\rho c_p)_f \varepsilon\right]\left(\frac{\partial T}{\partial \tau} + v_j \frac{\partial T}{\partial x_j}\right) = \frac{\partial}{\partial x_i}\left[(k_s(1-\varepsilon) + k_f \varepsilon)\frac{\partial T}{\partial x_i}\right] + Q. \tag{3}$$

Due to the small grain size of the adsorbent material, it was necessary to simplify the bed by using a porous medium, i.e., by adding a negative

momentum source term to the standard momentum conservation equation:

$$S_i = -\left(\sum_{j=1}^{3}\frac{1}{\alpha}\mu v_j + \sum_{j=1}^{3}C\frac{1}{2}\rho|v|v_j\right). \tag{4}$$

The source term S_i consists of two parts: viscous losses (classical Darcy's law, the first part of the right-hand side of Eq. (1)) and inertial losses (the second part of the right-hand side of Eq. (1)). The essence of replacing real structures with a porous medium is to determine their equivalent characteristics [16]. In laminar flows through porous media, the pressure drop is usually proportional to the velocity, and the inertial resistance C is equal to 0. The viscous resistance $1/\alpha$ was determined from the transformed Blake-Kozeny equation

$$\alpha = \frac{D_p^2}{150}\frac{\varepsilon^3}{(1-\varepsilon)^2}, \tag{5}$$

assuming a bed particle diameter of $D_p = 35 \times 10^{-5}$ m. The porosity $\varepsilon = 0.37$ was determined as the ratio of free space in the bed to its total volume. In a result, viscous resistance amounted to 9.60×10^9 m^{-2}

Water vapor was used as a fluid and silica gel was used as the solid body material. The adsorption process kinetics were modeled using the linear driving force (LDF) model [17], which takes into account the influence of mesopore and micropore structures. The form of the equation modified by Sun and Chakraborty [18] was used to incorporate the adsorption isotherms and activation energy:

$$S_m = \frac{\partial a}{\partial \tau} = k_m\left(a_{eq} - a\right), \tag{6}$$

where a is the amount of adsorbed water vapor in grams of water vapor per gram of bed and a_{eq} is the equilibrium value for the given conditions. The k_m coefficient depends on the bed parameters and is defined by

$$k_m = \frac{15 D_e}{r_a^2}, \tag{7}$$

where r_a is the radius of the adsorbent particle. The effective diffusion coefficient, D_e, which includes both surface and pore diffusion, is related to the isotherm:

$$D_e = D_0 \exp\left(-\frac{E_a}{RT}\right), \tag{8}$$

where $D_0 = 2.54 \times 10^{-4}$ m^2/s, $E_a = 42$ kJ/mol is the activation energy, R is the gas constant, and T is the temperature. Equation (6) was also used as a source term in the water vapor mass conservation equation (Eq. (1)).

The equilibrium concentration a_{eq} of the adsorbed water vapor was described by the Dubinin-Astakhov adsorption isotherm. This equation is frequently used for silica gel-water vapor systems and was originally developed based on Polanyi's adsorption theory, taking various forms [8, 19]. The model used in this study employed an equation based on the saturation pressure and temperature of the adsorbent:

$$\frac{a}{a_{eq}} = 0.37 \exp\left[-\left(\frac{RT}{E}\ln\frac{P_v}{P_s}\right)^n\right], \tag{9}$$

where P_v is the absolute pressure of water vapor, P_s is the saturation pressure for a given temperature, R is the gas constant, and the isothermal parameters n and E take values of 1.15 and 4280 J/mol, respectively.

Thermal effects were modeled as an energy source term Q, according to Eq. (10)

$$Q = H\frac{\partial a}{\partial \tau}, \tag{10}$$

where H is the heat of adsorption equal to 2415 kJ/kg.

The Green-Gauss node based gradient calculation scheme and the QUICK (quadratic upstream interpolation for convective kinematics) momentum, density, and energy discretization schemes (a high-order scheme for Cartesian grids) were used. The calculations were performed using a pressure-based solver with the PISO (pressure-implicit with splitting of operators) scheme. First order implicit transient formulation was applied.

The water vapor inlet was modeled as a pressure boundary condition with a absolute pressure $P_v = 1230$ Pa and an incoming temperature $T_v = 283.15$ K. The initial conditions were $T = 331.15$ K, $P = 1230$ Pa, and $a = 0.054$ kg/kg.

Iterative calculations were then carried out for 2000 time steps. Each time step lasted 1 s and consisted of a maximum of 30 iterations until the normalized residuals decreased by 4 orders of magnitude. In addition, the average vapor velocity at the inlet, the average temperature in the adsorption bed, and the amount of water vapor adsorbed by the bed were monitored to confirm iterative convergence.

In Figs. 4a and 4b, as well as 5a and 5b, different scales were used to clearly visualize the temperature distribution and saturation within the

adsorption bed. Figures 4a and 4b show the temperature distributions in the adsorption bed at $\tau = 200$ s and 2000 s, respectively. In the initial phase of the adsorption process (Fig. 4a), the highest temperature was found in the middle and upper parts of the bed, reaching approximately 323 K. The lowest temperature was observed in the lower part of the bed, at 305 K. This is because adsorption is an exothermic process and generates a large amount of heat throughout the volume of the bed in the initial stages, while the lower part of the bed was being cooled most intensively by the heat exchanger. At 2000 s (Fig. 4b), the adsorption proceeded with much lower intensity, and the coolest spot (300 K) was in the upper part of the bed, where $T_v = 283.15$ K was introduced due to the pressure difference between the bed and the evaporator. The temperature on the lower surface of the bed was approximately 303 K. The highest temperature, approximately 304 K, was observed in the middle part of the bed, where the adsorption process generated more heat than the cooling effect of the cooling medium.

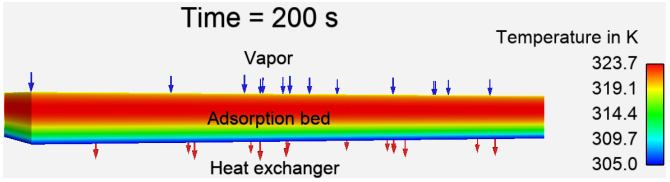

(a)

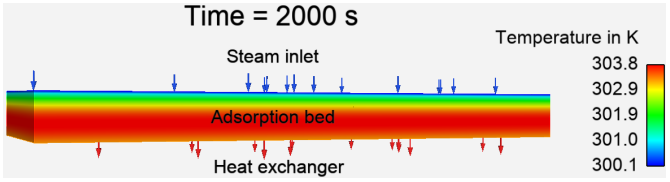

(b)

Figure 4: Graphical distribution of temperature in the adsorption bed at: (a) $\tau = 200$ s, (b) $\tau = 2000$ s.

At time $\tau = 200$ s of simulation, the largest amount of adsorbed vapor was observed in the lower part of the bed (Fig. 5a), as the heat exchanger cooling action locally intensified the adsorption. After 2000 s more uniform distribution of adsorbed water vapor is observed, with maximum in the upper part of the bed (Fig. 4b). This is again due to thermal effects (compare with Fig. 4b), also the top surface is more easily accessible to the water vapor.

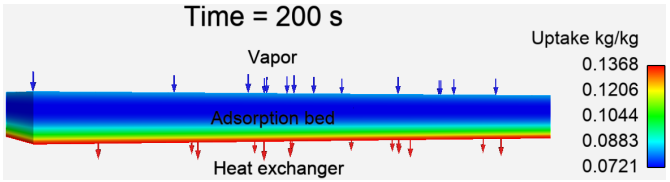

(a)

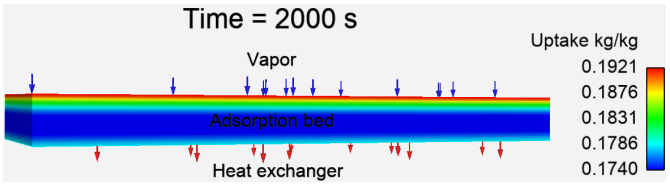

(b)

Figure 5: Graphical distribution of adsorbed vapor at: (a) $\tau = 200$ s, (b) $\tau = 2000$ s.

Model validation is presented in Fig. 6. The amount of water vapor adsorbed by the bed and the average bed temperature was compared between the simulation and experimental data [14].

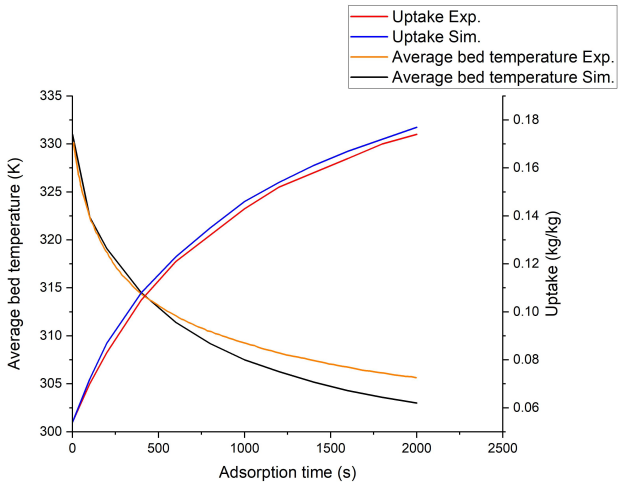

Figure 6: Comparison of experimental and numerical results: average bed temperature and the amount of adsorbed water vapor in the bed.

The maximum relative error between numerical simulation and experimental data for vapor uptake was 3%. For temperature, the maximum relative

error was 1%. Discrepancies may be attributed mostly to the uncertainty of experimental data and modelling assumptions (thermal equilibrium assumption, boundary conditions). The discrepancies were judged as small enough to use the developed model to analyze the influence of various factors on mass and heat transfer in the adsorption bed.

In this work, an analysis was performed on how the temperature of the cooling medium affects the sorption capacity of the bed. Several simulations were conducted at different temperatures of the cooling water (293–313 K), monitoring the change in vapor uptake (Fig. 7).

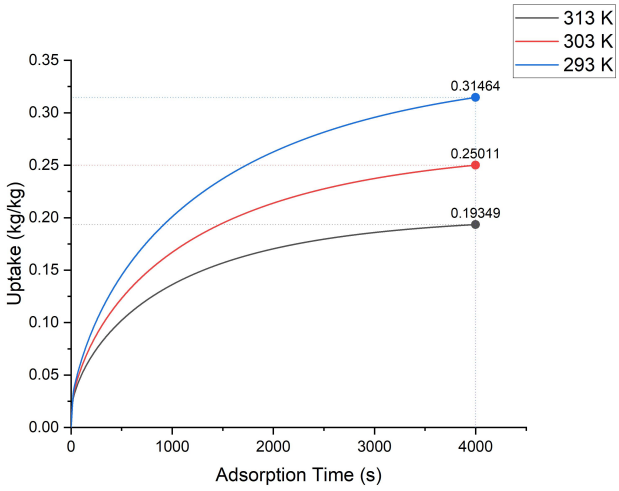

Figure 7: Comparison of the amount of vapor adsorbed by the bed at different cooling water temperatures.

The highest amount of water vapor was adsorbed at the lowest tested temperature (293 K), and the least at the highest tested temperature (313 K), with a difference of 0.121 kg/kg, which is in accordance with adsorption theory and implemented isotherms. This is particularly important considering the availability of cooling medium in different applications and geographic locations. In areas with warm climates where it might not be possible to obtain cooling water for the bed below 303 K using fan-cooling, the device efficiency would already decrease at the design stage due to the lower saturation achievable during each cycle.

In adsorption refrigeration systems, the adsorption and desorption processes occur alternately between two beds, so their time must be equal. The next step was to investigate how the temperature of hot water affects

the desorption process (Figs. 8–10). For this purpose, the bed regeneration process was simulated, starting from saturation condition. The initial degree of sorbent saturation, which largely depends on the temperature of the cooling medium, as shown in Fig. 7, significantly affects the course of the desorption process.

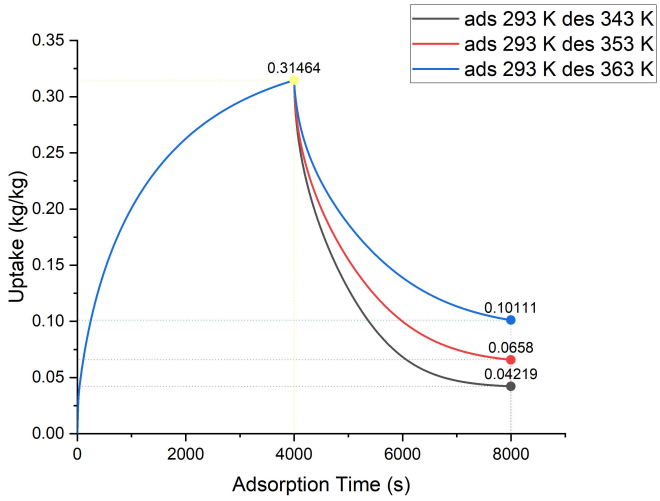

Figure 8: Comparison of the amount of vapor desorbed by the bed at different temperatures of the heating water.

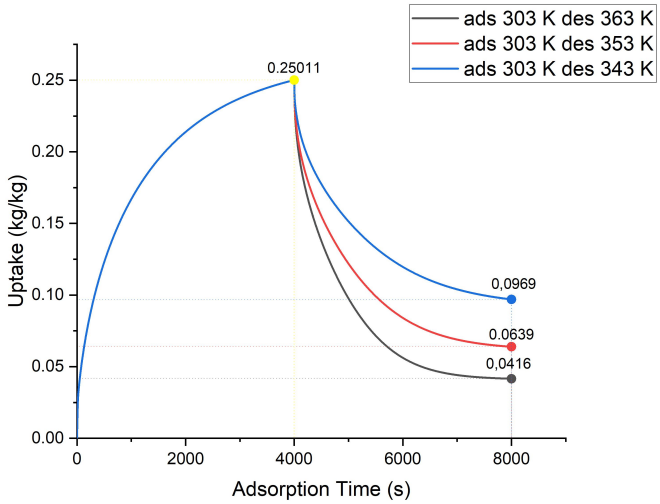

Figure 9: Comparison of the amount of vapor desorbed by the bed at different temperatures of the heating water.

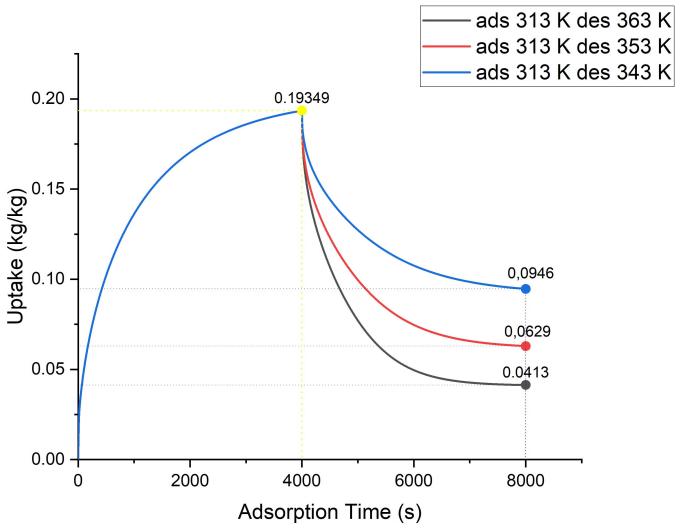

Figure 10: Comparison of the amount of vapor desorbed by the bed at different temperatures of the heating water.

The lowest vapor uptake at the end of the desorption cycle was achieved when the adsorption process was powered by cooling water at $T_c = 313$ K and regenerated with heating water at $T_h = 363$ K, which amounted to 0.0413 kg/kg. The highest amount of adsorbed vapor, 0.1011 kg/kg, remained within the sorbent grains when the bed was cooled with $T_c = 293$ K during the adsorption process and desorption was carried out at a temperature of 343 K.

The relationship between these two processes is significant, as the more vapor remains in the adsorbent material after the regeneration process, the less it can adsorb in the subsequent adsorption process. Also, the adsorption process is more intense the further the bed is from the saturation point. This means that in regions with a warm climate it is possible to achieve higher temperatures of hot water used for bed regeneration. This will result in a lower degree of bed saturation, which will compensate for the higher temperature of the cooling water during the adsorption process. This indicates the possibility of utilizing external conditions during the device design process.

The course of the adsorption/desorption process was analyzed for various single-cycle times of 4000, 6000, and 8000 s and the results are shown in Fig. 11. The analysis was performed for the case where the cooling water

temperature during the adsorption process was 303 K, while the hot water temperature during the desorption process was 353 K.

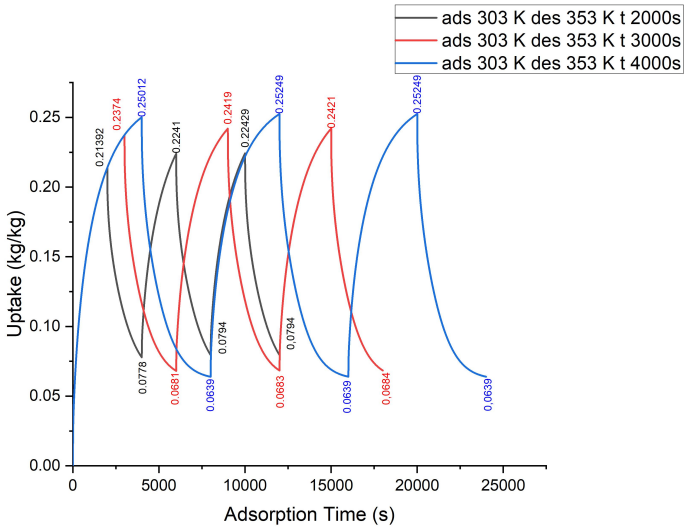

Figure 11: Comparison of the vapor uptake for cooling water temperature of 303 K, heating water temperature of 353 K and for various cycle lengths.

Assuming zero uptake as an initial condition, the degree of saturation at key moments (beginning of adsorption and beginning of desorption) reaches equilibrium after about 3 cycles for cases where the single cycle time was $\tau_{sc} = 4000$ s and 6000 s, respectively. For the case where $\tau_{sc} = 8000$ s, stability was achieved after only 2 cycles. Shortening the single cycle time of the device increases the number of cycles required to stabilize the saturation of the adsorbent bed.

In the case of refrigeration devices, the intensity with which water vapor is adsorbed by the adsorption bed is important, because it affects the device's efficiency. In the case of the third cycle, where adsorption processes reached stability, the amount of absorbed water vapor (the difference in saturation level between the beginning and end of adsorption) in the adsorbent bed was 0.1449 kg/kg for $\tau_{sc} = 4000$ s, 0.1737 kg/kg for $\tau_{sc} = 6000$ s, and 0.1885 kg/kg for $\tau_{sc} = 8000$ s.

Increasing the duration of the adsorption process from 2000 s to 3000 s resulted in an increase of the amount of absorbed water vapor by 0.0228 kg/kg. Increasing the duration of the adsorption process from 3000 s to 4000 s resulted in an increase in the amount of absorbed water vapor

by only 0.0148 kg/kg. The increase in adsorbed water vapor was almost twice as low when extending the time from 3000 s to 4000 s compared to extending the time from 2000 s to 3000 s.

Differences can also be observed on the adsorption and desorption graph where the single cycle duration is 4000 s (Fig. 12). The amount of adsorbed vapor in the third cycle during the first 1000 s of the adsorption process (from 8000 s to 9000 s) is 0.108 kg/kg, while in the subsequent 1000 s (from 9000 s to 10000 s) it decreases to 0.0361 kg/kg. This indicates that the intensity of the adsorption process significantly decreases with the duration of the process.

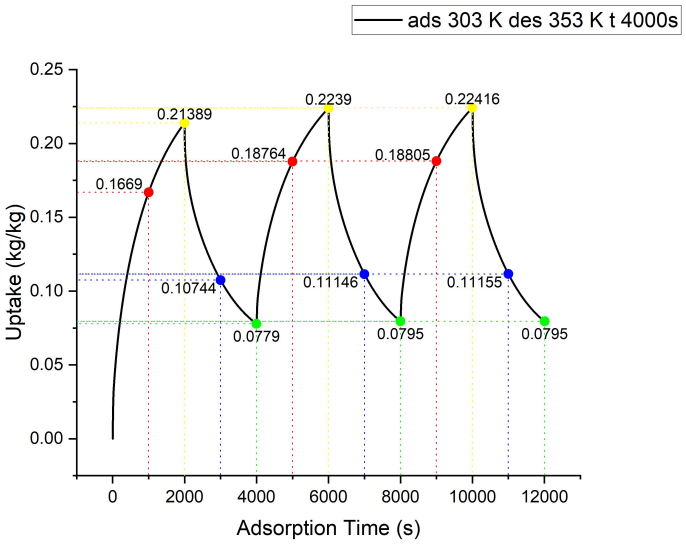

Figure 12: Vapor uptake in function of time for cooling water temperature of 303 K and heating water temperature of 353 K, for cycle lengths of 4000 s.

The effect of the duration of the adsorption process on its course is due to the degree of saturation of the bed. This means that the optimal cycle duration depends on the intensity of the process (cooling water temperature of the bed during the adsorption process), the initial degree of saturation (heating water temperature of the bed during the desorption process), and the type of adsorbent-adsorbate pair. It should be remembered that the main task of the adsorption process in adsorption refrigeration devices is to maintain a low evaporation temperature by extracting the vapor generated in the evaporator. Therefore, the main criterion for selecting the cycle

duration of the adsorption/desorption process is the minimum amount of vapor that can be adsorbed at any given time corresponding to the amount of vapor generated at the same time in the evaporator.

3 Summary

The article presents a method for modeling mass and heat transfer in an adsorption bed using CFD methods. The proposed equation implementation approach is universal for modeling adsorption processes, while the kinetic and equilibrium equations used are specific to the analyzed type of silica gel. The calculations obtained using the model were in agreement with the experimental results available in the literature. The presented approach will be the basis for further experimental research.

Numerous scenarios were tested numerically. The study of the influence of the cooling and heating temperatures on the adsorption/desorption process showed the significance of these parameters and indicated the possibility of utilizing external conditions during the device design process. The impact of cycle length on the intensity of absorbed vapor was also analyzed. Cycles with a duration of 4000 s, 6000 s, and 8000 s were tested. It was demonstrated that the intensity of the adsorption process significantly decreases with the duration of the process. By doubling the cycle length from 4000 s to 8000 s, the amount of adsorbed vapor increased by only 23%.

The developed numerical model allows for the selection of optimal cycle times for adsorption refrigeration devices under specific conditions, which can translate into improving their COP cooling efficiency. This, in turn, can contribute to their competitiveness in the market and environmental protection.

Acknowledgments

The paper was prepared as part of the research and development activities of M.A.S. Sp. z o.o. implementing projects: POIR.01.01.01-00-0628/19 “Development of an innovative, multi-module chiller with increased energy efficiency” and POIR.02.01.00-00-0172/19 “M.A.S. R&D Center of Innovative, Environmentally-Friendly Devices and Systems for Cooling and Energy Storage”.

Received 13 March 2023

References

[1] International Energy Agency (IEA: *The future of cooling opportunities for energy-efficient air conditioning*, 2018. https://iea.blob.core.windows.net/assets/0bb45525-277f-4c9c-8d0c-9c0cb5e7d525/The_Future_of_Cooling.pdf (accessed 18 Aug. 2022).

[2] Fan Y., Luo L.: *Review of solar sorption refrigeration technologies: Development and applications*. Renew. Sust. Energ. Rev. **11**(2007), 8, 1758–1775.

[3] Wang D., Li H., Li D., Xia Y., Zhang J.: *A review on adsorption refrigeration technology and adsorption deterioration in physical adsorption systems*. Renew. Sust. Energ. Rev. **14**(2010), 1, 344–353.

[4] Kuchmacz J., Bieniek A., Mika Ł.: *The use of adsorption chillers for waste heat recovery*. Polityka Energetyczna – Energ. Policy J. **22**(2019), 2, 89–106.

[5] Krzywanski J., Sztekler K., Bugaj M., Kalawa W., Grabowska K., Chaja P., Sosnowski M., Nowak W., Mika Ł., Bykuć S.: *Adsorption chiller in a combined heating and cooling system: simulation and optimization by neural networks*. Bull. Pol. Acad. Sci. Tech. Sci. **69**(2021), 3, e137054.

[6] Li X., Hou X., Zhang X., Yuan Z.: *A review on development of adsorption cooling – Novel beds and advanced cycles*. Energ. Convers. Manage. **94**(2015), 221–232.

[7] Elsheniti M.B., Elsamni O.A., Al-Dadah R.K., Mahmoud S., Elsayed E., Saleh K.: *Adsorption refrigeration technologies*. In: Sustainable Air Conditioning Systems. IntechOpen, 2018.

[8] Wang R., Wang L., Wu J.: *Adsorption Refrigeration Technology – Theory and Application*. Wiley, 2014.

[9] Rani S., Sud D.: *Effect of temperature on adsorption-desorption behaviour of triazophos in Indian soils*. Plant Soil Environ. **61**(2015), 1, 36–42.

[10] Papakokkinos G., Castro J., López J., Oliva A.: *A generalized computational model for the simulation of adsorption packed bed reactors – Parametric study of five reactor geometries for cooling applications*. Appl. Energ. **235**(2019), 409–427.

[11] Petrik M., Szepesi G., Jármai K.: *CFD analysis and heat transfer characteristics of finned tube heat exchangers*. Pollack Period. **14**(2019), 3, 165–176.

[12] Wang X., Chua H., Ng K.: *Simulation of the silica gel-water adsorption chillers*. In: Proc. Int. Refrigeration and Air Conditioning Conf., July 12-15, 2004, 663.

[13] White J.: *A CFD Simulation on how the different sizes of silica gel will affect the adsorption performance of silica gel*. Model. Simul. Eng. **2012**(2012), 65143.

[14] Mohammed H.: *Assesment of numerical models in the evaluation of adsorption cooling system performance*. Int. J. Refrig. **99**(2019), 166–175.

[15] Ansys Fluent Theory Guide, 2023, https://www.ansys.com/

[16] Śmierciew K.: *Numerical and Experimental Aspects of Selected Thermal and Flow Problems of Equipment Used in Refrigeration and Thermal Technology*. Oficyna Wydawnicza Politechniki Białostockiej, Białystok 2018 (in Polish).

[17] Glueckauf E.: *Theory of chromatography. Part 10 – formula for diffusion into spheres and their application to chromatography.* Trans. Faraday Soc. **51**(1955), 1540–1551.

[18] Sun B., Chakraborty A.: *Thermodynamic frameworks of adsorption kinetics modeling: dynamic water uptakes on silica gel for adsorption cooling applications.* Energy **84**(2015), 296–302.

[19] Tran H.: *Mistakes and inconsistencies regarding adsorption of contaminants from aqueous solutions: A critical review.* Water Res. **120**(2017), 88–116.